J. Chem. Sci. (2019) 131:122
https://doi.org/10.1007/s12039-019-1713-7

REVIEW ARTICLE

Special Issue on 150 years of the Periodic Table

On the position of La, Lu, Ac and Lr in the periodic table: a perspective

ADITI CHANDRASEKAR[a], MEENAKSHI JOSHI[b,c] and TAPAN K GHANTY[b,c,*]
[a]Department of Inorganic and Physical Chemistry, Indian Institute of Science, Bangalore 560 012, Karnataka, India
[b]Theoretical Chemistry Section, Chemistry Group, Bhabha Atomic Research Centre, Mumbai 400 085, Maharashtra, India
[c]Homi Bhabha National Institute, Training School Complex, Anushakti Nagar, Mumbai 400 094, Maharashtra, India
E-mail: tapang@barc.gov.in

MS received 30 October 2019; revised 5 November 2019; accepted 6 November 2019; published online 5 December 2019

Abstract. The periodic table of elements, organised as blocks of elements that contain similar properties, occupies a central role in chemistry. However, the position of some of the elements in the periodic table is a debate that has been ensuing over the past one and a half long centuries. Particularly, the positions of lanthanum (La), lutetium (Lu), actinium (Ac) and lawrencium (Lr) in the periodic table have been quite controversial. Different kinds of studies carried out by various research groups have yet left the fate of these elements undecided as the results of these investigations suggested that these elements could potentially be placed in the d-block, p-block or all four in the f-block. Our recent work looked into this question from a new perspective, involving encapsulation of La, Lu, Ac and Lr into Zintl ion clusters, Pb_{12}^{2-} and Sn_{12}^{2-}. These clusters were chosen as they provide a fitting environment for the determination of structural, thermodynamic and electronic properties of the encapsulated species. Various results that have been evaluated and subsequently analysed (Joshi *et al.* in *Phys. Chem. Chem. Phys.* 20:15253–15272, 2018) in order to seek out similarities and differences for making justified conclusions about the placement of all these four elements in the periodic table are the subject matter of this review article.

Keywords. Lanthanide; actinide; f-block elements; density functional calculations; periodic table.

1. Introduction

One of the most long-lasting questions in the last century to this has been a deceptively trivial one; the positions of lutetium (Lu), lawrencium (Lr), lanthanum (La) and actinium (Ac) in the modern periodic table. As trivial as it may sound, this problem has been the cause of heated scientific debate and the answers to this question provided by various research groups are in the least agreement with each other. Way back in the 1980s Jensen suggested that La and Ac should belong to the f block and Lu and Lr in the d block.[1] Jensen proposed that the right place for Lu, is in the third group of the periodic table below scandium (Sc) and yttrium (Y). The reasons for such a placement were the absence of empty f-orbitals in Lu, along with its similar periodic trends to Sc and Y in terms of atomic radii, the sum of the first two ionization potentials, the melting point, and electronegativity. Jensen also assigned Lr to group 3 and below Lu solely based on their similar electronic configuration.[1,2] This arrangement that resulted in fourteen-element rows for the f-block elements i.e., La–Yb and Ac–No is the version adopted by Wikipedia. Subsequent calculations incorporating the relativistic effect, revealed the ground state of Lr to be $[Rn]5f^{14}7s^27p^1$ instead of $[Rn]5f^{14}6d^17s^2$.[3–5] On this basis, in stark opposition to Jensen, Lavelle proposed that the La and Ac be placed in the d block while Lu and Lr must be in the f block.[6] In 2008, Lavelle claimed that Lr and Lu must not be placed in the d block, but rather that La ($[Xe]5d^16s^2$) and Ac($[Rn]6d^17s^2$) be placed in the d block owing to their last electron being in a d orbital. Lavelle, hence maintained the view that Lu and Lr should remain in the f block[6–8] which would still consist of fourteen-

*For correspondence

element rows, Ce–Lu and Th–Lr. The suggestion of Lavelle has been accepted by the Royal Society of Chemistry as well as the American Chemical Society. In addition to these conflicting views with their justifications from both sides, a third proposition emerged in as recently as 2016 from Pyykkö and coworkers[9] who concluded that all the elements La–Lu and Ac–Lr are best fitted in 15-element rows in the f block consisting of lanthanides and actinides, respectively. The first ionization potential of Lr has been experimentally and theoretically calculated (4.96 eV) and found to be of an exceptionally low value considering the large number of protons in its nucleus.[10] However, this leads one to the importance of the relativistic effects, particularly while considering the heavy elements.[10] Pyykkö *et al.,* in 2016, employed the relativistic electronic configuration of Lr([Rn]$5f^{14}7s^27p^1$), to investigate the effect of the ground state configuration of Lr on its chemical behaviour. They concluded that both Lr and Lu show the same chemical behaviour though their ground state configurations vary. Nevertheless, Pyykkö *et al.,*[9] showed that Tl and Lr have different properties, despite them both possessing similar ground state np^1 configurations. In view of their results, Pyykko *et al.,* recommended the placement of all lanthanides (La–Lu) and actinides (Ac–Lr) in the f block[9] which will then consist of 15 elements with configurations from f^0 to f^{14} instead of the conventional 14-element f-block. This scheme has been adopted in the modern periodic table as well as by IUPAC.[11] In effect, these controversies have led to a lack of clarity about the position of Lr, Lu, La and Ac in the periodic table, and this issue remains unresolved till date. In our recent work,[12] this issue has been addressed by employing encapsulated $M@Pb_{12}^{2-}$ and $M@Sn_{12}^{2-}$ clusters (M = Lr^n, Lu^n, or La^{3+}, Ac^{3+} where n = 0, 1, 2, 3) as model systems to provide in-depth insights into this long-drawn controversy. Thus, structural, thermodynamic and electronic properties of these clusters were studied using density functional theory (DFT) in order to seek out their similarities and differences in a manner such that conclusions can be drawn about the placement of these elements in the periodic table.[12] The present article is a brief perspective based on these results.

2. Computational methods

All the DFT calculations have been carried out[12] using the TURBOMOLE-6.6[13] and ADF 2016[14,15] programs. Optimizations have been performed using the Perdew–Burke–Ernzerhof (PBE) functional[16] in conjunction with the def-TZVP basis set which has been used along with a relativistic effective core potential (RECP) for all the heavier elements *viz.*, Pb (ECP 78), Sn (ECP 46), Ac (ECP 60), Lr (ECP 60) and Lu (ECP 28).[17–23] For La, the def2-TZVP basis set has been used during the calculations along with ECP 46. Further details are given in Ref [12].

3. Choosing encapsulated clusters of tin and lead as model systems

Following the discovery of fullerene (C_{60} cluster), new avenues opened in the area of cluster research.[24–29] Its unique truncated icosahedral structure possessing a large diameter of 7 Å enables the C_{60} cluster to accommodate a wide selection of atoms or ions within it. This leads to the creation of "doped clusters" with applications in different areas of science including biology, nanotechnology and medicine.[24–29] Such clusters when doped with atoms or ions have been known to display useful electronic, magnetic and chemical properties including catalytic activity.[30–32] Apart from clusters of carbon, other elements have since evolved in the emerging field of cluster research. Several of these have been theoretically been conceived and a subset of these has been experimentally synthesised. Twelve atom clusters of tin and lead known as "stannaspherene" (Sn_{12}^{2-})[33] and "plumbaspherene" (Pb_{12}^{2-}),[34] respectively were experimentally realised in 2006 by Cui *et al.* Interestingly, both the Pb_{12}^{2-} and Sn_{12}^{2-} clusters are similar to fullerene in that they have spherical pi bonding as well as an empty cage with relatively large diameters of 6.3 Å and 6.1 Å, respectively, which are only marginally shorter than the internal diameter of the C_{60} cage (7 Å). Thus, a variety of transition metal and lanthanide encapsulated clusters of Pb_{12}^{2-} and Sn_{12}^{2-} have been investigated experimentally.[35–42] Thus, there is a plethora of captivating metal atom or ion encapsulated Si_n^-, Ge_n^-, $Sn_n^-$and Pb_{12}^{2-} clusters that have been experimentally and theoretically examined.[43–58] A few examples include kinetically stable noble gas atom or dimer (H_2 and He_2) encapsulated Pb_{12}^{2-} and Sn_{12}^{2-} clusters which have been predicted by our group.[59] Addressing the point of stability, it has additionally been shown that encapsulated Pb_{12}^{2-} and Sn_{12}^{2-} clusters preserved their structural integrity even at high temperatures of 700 K.[59] Delving further, considering their similar cage sizes, the possibility of having an $Lr@C_{60}$ cluster[60] makes the prediction of Lr or Lu encapsulated Pb_{12}^{2-} and Sn_{12}^{2-} clusters realisable.

4. Structure and binding energy

We have extensively investigated $M@Pb_{12}^{2-}$ and $M@Sn_{12}^{2-}$ clusters (M = Lr^{n+}, Lu^{n+}, La^{3+} and Ac^{3+} where n = 0, 1, 2, 3) using density functional theory (DFT). With the sole objective to determine the position of these four elements in the periodic table, the similarities or dissimilarities in their electronic, structural and thermodynamic properties have been extensively discussed.[12] The synthesis of $M@Pb_{12}^{2-}$ and $M@Sn_{12}^{2-}$ clusters could well be made possible through photoelectron spectroscopy, as $Lu@Ge_n^-$[44] and $M@Si_n^-$ (n = 6–20)[43] clusters have already been prepared experimentally. We have mainly focused on the metal encapsulated Pb_{12}^{2-} and Sn_{12}^{2-} clusters in which the metal ions exist in their most stable oxidation state of +3 *viz.,* Lu^{3+}, Lr^{3+}, La^{3+} and Ac^{3+}. However, in order to make an effective comparison with the +3 state, other charged $M@Pb_{12}^{2-}$ and $M@Sn_{12}^{2-}$ (M = Lr^{n+}, Lu^{n+}, n = 0, 1, 2) clusters have also been examined to the same extent with respect to structural, energetic, and electronic properties. Furthermore, in each case, the thermodynamic property of the binding energy during the encapsulation process has also been analyzed. Interestingly, all $M@Pb_{12}^{+}$ and $M@Sn_{12}^{+}$ (M = Lr and Lu) clusters were found to be stable 18-bonding-electron systems with shell closing.

First, we have investigated the icosahedral geometry for the bare Pb_{12}^{2-} and Sn_{12}^{2-} cages which is the global minimum structure of the bare Pb_{12}^{2-} and Sn_{12}^{2-} cages.[33,34,61] Metal encapsulated various 13-atom clusters with closed-shell configurations have been shown experimentally and theoretically to possess an icosahedral structure as their ground state geometry.[30,38,39,41,42,62,63] The addition or removal of electrons to this closed-shell configuration of the clusters reduces the symmetry.[53,64] We have predicted various structures for the metal-doped clusters in different oxidation states. The optimized minimum energy geometries of the encapsulated clusters $M@Pb_{12}^{2-}$ and $M@Sn_{12}^{2-}$ (M = Lr^{n+}, Lu^{n+} n = 0, 1, 2, 3) are shown in Figure 1 and their relative energies with respect to the most stable geometry in each oxidation state of Lr and Lu are listed (Table 1). The binding energy is a guiding parameter indicating the stability of the clusters. All the binding energies of Lr and Lu encapsulated Pb_{12}^{2-} and Sn_{12}^{2-} clusters are negative (Table 2) indicating that they are thermodynamically stable. In every case, a decrease in the charge on the

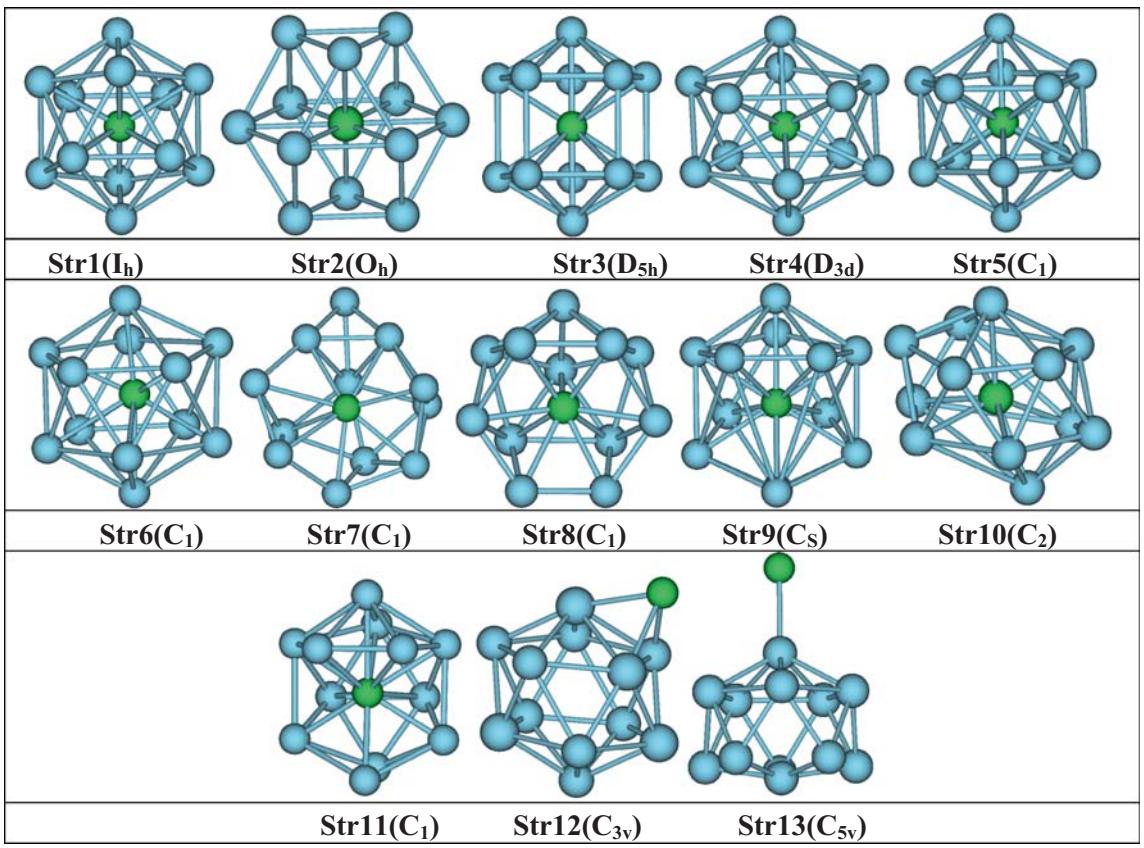

Figure 1. Optimized structures of $M@Pb_{12}^{2-}$ (M = Lr^{n+}, Lu^{n+} and n = 0, 1, 2, 3) clusters (Reproduced from Ref.[12] with permission from the Royal Society of Chemistry).

Table 1. Relative Energy (RE in eV) of various isomers of $M@E_{12}^{2-}$ (M = Lr^{n+}, Lu^{n+}, E = Pb, Sn and n = 0, 1, 2, 3) Clusters.[a,b]

Geometry	RE		Geometry	RE	
	$Lr^n@Pb_{12}^{2-}$	$Lu^n@Pb_{12}^{2-}$		$Lr^n@Sn_{12}^{2-}$	$Lu^n@Sn_{12}^{2-}$
$M@E_{12}^{+}$					
Str1(I_h)	0.000	0.000	Str1(I_h)	0.000	0.000
Str2(O_h)	2.127[c]	2.225[c]	Str2(O_h)	1.830[c]	1.938[c]
Str3(D_{5h})	2.755[c]	2.861[c]	Str3(D_{5h})	2.309[c]	2.397[c]
Str12(C_{3v})(exo)	1.331	2.096	Str12(C_{3v})(exo)	0.516	1.331
Str13(C_{5v})(exo)	2.060[c]	3.550[c]	Str13(C_{5v})(exo)	1.161[c]	2.765[c]
$M@E_{12}$					
Str4(D_{3d})	0.000	0.000	Str4(D_{3d})	0.000	0.011
Str5(C_1)	0.011	0.010	Str6(C_1)	0.042	0.000
Str6(C_1)	0.015	0.009	Str7(C_1)	0.556	0.967
Str7(C_1)	1.824	1.607			
$M@E_{12}^{-}$					
Str8(C_1)	0.000	0.000	Str8(C_1)	0.000	0.000
Str9(C_s)	0.222	0.185	Str6(C_1)	0.724	0.546
Str4(D_{3d})	0.384	0.184	Str12(C_1)	0.422	0.393
Str7(C_1)	1.216	1.329	Str7(C_1)	1.173	0.781
$M@E_{12}^{2-}$					
Str10(C_2)	0.000	0.000	Str8(C_1)	0.000	0.000
Str8(C_1)	0.009	0.008	Str10(C_2)	0.142	0.202
Str7(C_1)	1.214	1.318	Str7(C_1)	1.031	0.861

[a]Symmetry of each isomer is given in the parenthesis.

[b]All results are taken from Ref.[12] with permission from the Royal Society of Chemistry.

[c]Clusters are associated with imaginary frequencies.

Table 2. Binding Energy (BE, in eV) of $M@E_{12}^{2-}$ (M = Lr^{n+}, Lu^{n+}, La^{3+}, Ac^{3+}, E = Pb, Sn and n = 0, 1, 2, 3) Clusters.[a]

$M@Pb_{12}^{2-}$	Geometry	BE	$M@Sn_{12}^{2-}$	Geometry	BE
$Lu@Pb_{12}^{+}$	Str1(I_h)	− 37.90	$Lu@Sn_{12}^{+}$	Str1(I_h)	− 37.03
$Lr@Pb_{12}^{+}$	Str1(I_h)	− 37.19	$Lr@Sn_{12}^{+}$	Str1(I_h)	− 36.23
[b]$La@Pb_{12}^{+}$	Str1(I_h)	− 31.36	[b,c]$La@Sn_{12}^{+}$	Str1(I_h)	− 30.04
$Ac@Pb_{12}^{+}$	Str1(I_h)	− 28.88	[c]$Ac@Sn_{12}^{+}$	Str1(I_h)	− 27.47
$Lu@Pb_{12}$	Str4(D_{3d})	− 21.61	$Lu@Sn_{12}$	Str6(C_1)	− 21.16
$Lr@Pb_{12}$	Str4(D_{3d})	− 20.03	$Lr@Sn_{12}$	Str4(D_{3d})	− 19.57
$Lu@Pb_{12}^{-}$	Str8(C_1)	− 9.84	$Lu@Sn_{12}^{-}$	Str8(C_1)	− 10.21
$Lr@Pb_{12}^{-}$	Str8(C_1)	− 8.00	$Lr@Sn_{12}^{-}$	Str8(C_1)	− 8.30
$Lu@Pb_{12}^{2-}$	Str10(C_2)	− 3.67	$Lu@Sn_{12}^{2-}$	Str8(C_1)	− 4.32
$Lr@Pb_{12}^{2-}$	Str10(C_2)	− 2.79	$Lr@Sn_{12}^{2-}$	Str8(C_1)	− 3.37

[a]All results are taken from Ref.[12] with permission from the Royal Society of Chemistry.

[b]def2–TZVP basis set has been used for La atom in $La@Pb_{12}^{+}$ and $La@Sn_{12}^{+}$ clusters, while for remaining atoms def−TZVP basis set is used.

[c]Clusters are associated with imaginary frequencies.

encapsulated atom or ion is accompanied by a decrease in binding energy (Table 2). Hence, the greater the positive charge on the encapsulated metal ion, the higher is the interaction between the cage and the encapsulated atom (ion). Lr^{n+} encapsulated clusters in their different oxidation states (n = 0, 1, 2, 3) are associated with binding energies very similar to those of Lu^{n+} encapsulated clusters in the corresponding oxidation states in spite of the size difference between Lr and Lu. On comparing these energies with La and Ac clusters,[12] their binding energy is observed to be relatively smaller than Lr and Lu encapsulated

clusters (Table 2). The larger size of La and Ac reduces the stability of the system both in terms of bond length as well as accommodation in the cage.

5. Density of states and molecular orbital order

The density of states (DOS) plots for bare Pb_{12}^{2-} clusters are compared with those of $M@Pb_{12}^{+}$ (M = Lr and Lu) clusters (Figure 2(a)). Intense bands, which correspond to valence 6s, 6p and 5s, 5p orbitals are observed for both the bare and encapsulated clusters. However, the DOS of the corresponding peaks for the encapsulated clusters are slightly red-shifted compared to the bare Pb_{12}^{2-} cluster. However, our purpose is to draw comparisons between the encapsulated clusters and the Lu^{3+} and Lr^{3+} ion encapsulated Pb_{12}^{2-} clusters show almost similar energy shifts. A very similar density of states behaviour is shown by Lu^{3+} and Lr^{3+} ion encapsulated Pb_{12}^{2-} clusters.

Molecular orbital (MO) energy level diagrams of Lu^{3+} and Lr^{3+} ion encapsulated Pb_{12}^{2-} clusters (Figure 2(b)) show fairly large HOMO–LUMO energy gaps for $M@Pb_{12}^{+}$ clusters confirming their chemical stability in addition to the binding energies discussed above. Compared to the $M@Pb_{12}^{+}$ clusters a smaller HOMO–LUMO energy gap is observed for $M@Sn_{12}^{+}$ clusters (Figure 3). The smaller size of the Sn_{12}^{2-} cage marginally de-stabilises the encapsulated cluster in comparison to the corresponding Pb_{12}^{2-} cluster systems. Clusters in which the encapsulated Lr and Lu (Lr^{n+}, Lu^{n+} and n = 0, 1, 2) have positive charges less than +3 have lower HOMO–LUMO gaps. The

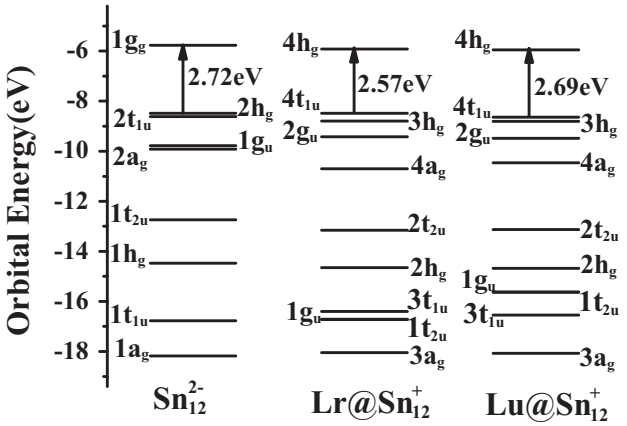

Figure 3. Molecular energy level diagram of bare Sn_{12}^{2-} and Lr^{3+} and Lu^{3+} encapsulated cluster. (Reproduced from Ref.[12] with permission from the Royal Society of Chemistry).

HOMO–LUMO energy gaps of Lu^{3+} and Lr^{3+} encapsulated Pb_{12}^{2-} and Sn_{12}^{2-} clusters are relatively higher than those for La^{3+} and Ac^{3+} encapsulated clusters. Thus, the more negative binding energies of the Lu^{3+} and Lr^{3+} encapsulated Pb_{12}^{2-} and Sn_{12}^{2-} clusters combined with the higher value of the HOMO–LUMO confirms the relatively higher stability of the Lu^{3+} and Lr^{3+} encapsulated clusters.

6. Electron counting rules and the stability of encapsulated clusters

The 18-electron rule[65,66] has been extensively employed in order to explain the stability of several systems; particularly transition metal complexes.[67,68]

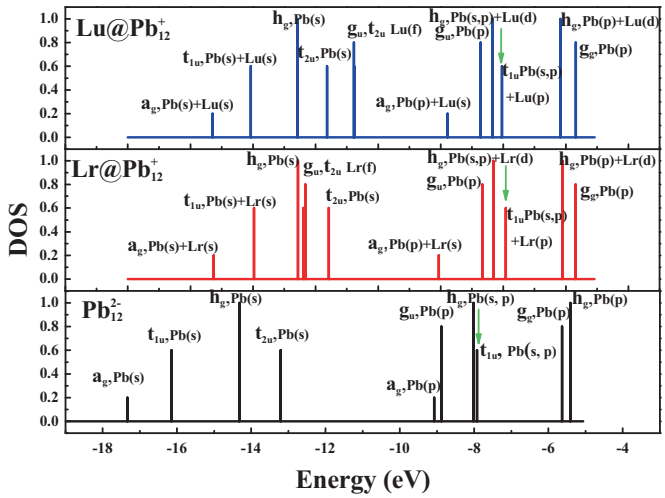

(a)

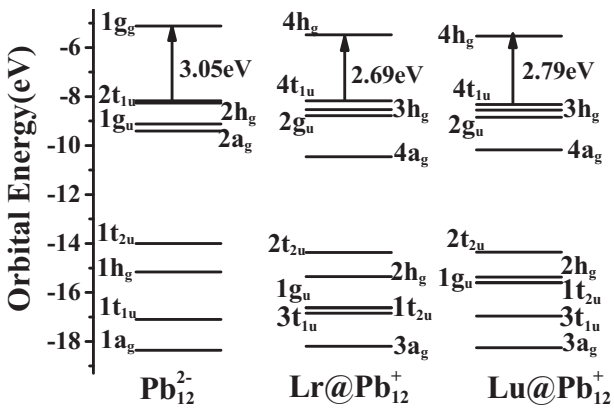

(b)

Figure 2. (a) The variation of density of states (DOS) and (b) Molecular energy level diagram of bare Pb_{12}^{2-} and Lr^{3+} and Lu^{3+} encapsulated cluster. The vertical green arrow is pointing toward HOMO. (Reproduced from Ref.[12] with permission from the Royal Society of Chemistry).

Beyond this purview, in the recent past the 18-electron counting rule has succeeded in explaining the stability of clusters such as $W@Au_{12}$ and $Sg@Au_{12}$.[62,63,69,70] However, for early lanthanide and actinide encapsulated clusters, the 32-electron rule holds more promise.[51,52, 71,75] In addition to the 18-electron and 32-electron rules, to explain the stability of main group metal atom/ion encapsulated gold clusters the 20-electron principle has also been invoked.[76]

The energy level diagram (Figure 2b and Figure 3) and MO pictures of the encapsulated clusters (Figures 4 and 5) reveal that $M@Pb_{12}^{+}$ and $M@Sn_{12}^{+}$ (M = Lr and Lu) systems follow the 18-electron rule with shell closing in $4t_{1u}$, $3h_g$ and $4a_g$ MOs corresponding to an $ns^2np^6(n-1)d^{10}$ configuration. From Figure 2b and Figure 3 it can be seen that in bare Pb_{12}^{2-} and Sn_{12}^{2-} there are four valence energy level corresponding to h_g, t_{1u}, g_u and a_g MOs. However, in metal-doped

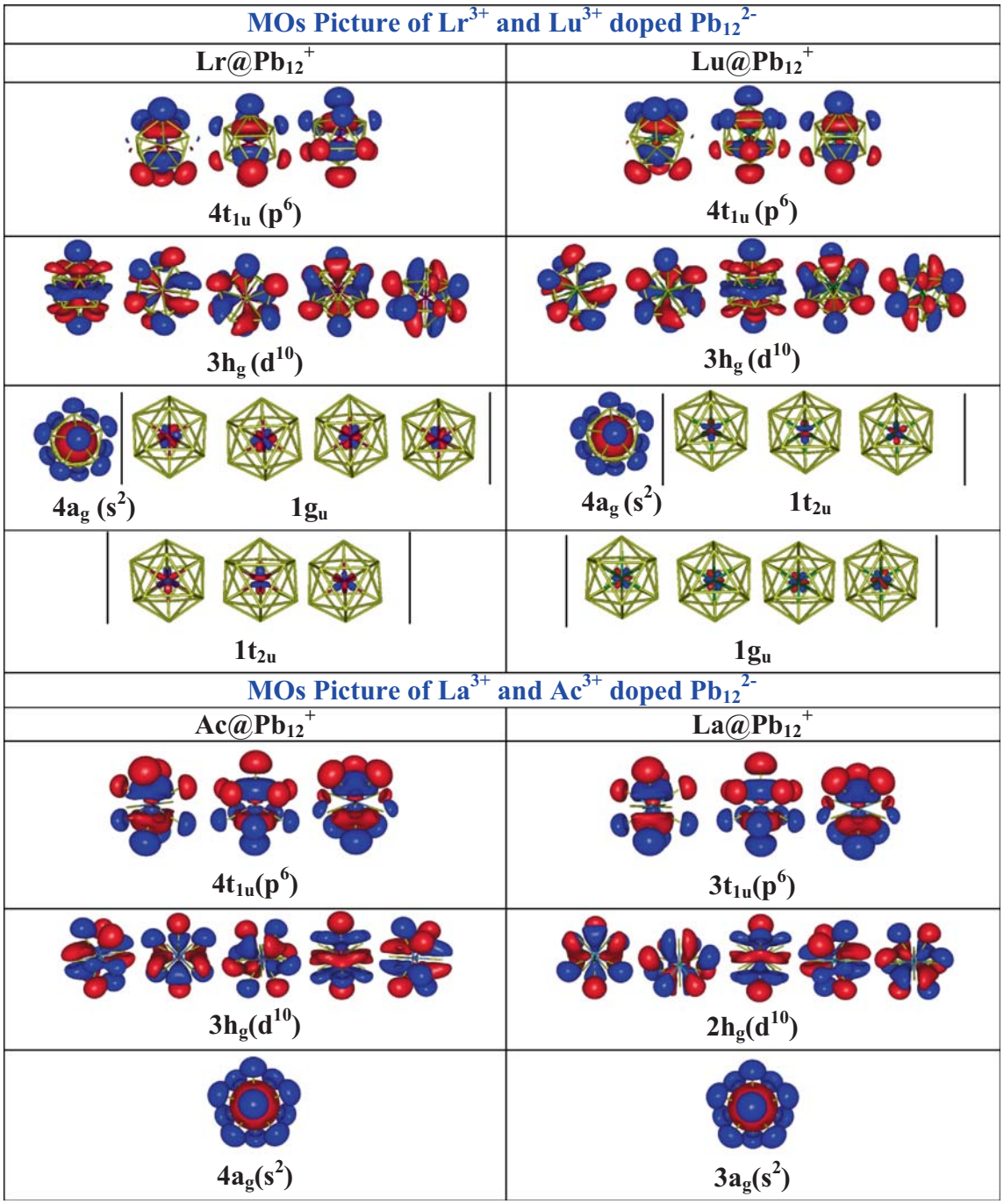

Figure 4. Molecular orbital pictures of $M@Pb_{12}^{+}$ clusters (M = Lr, Lu, Acand La) at PBE/DEF level of theory. (Reproduced from Ref.[12] with permission from the Royal Society of Chemistry).

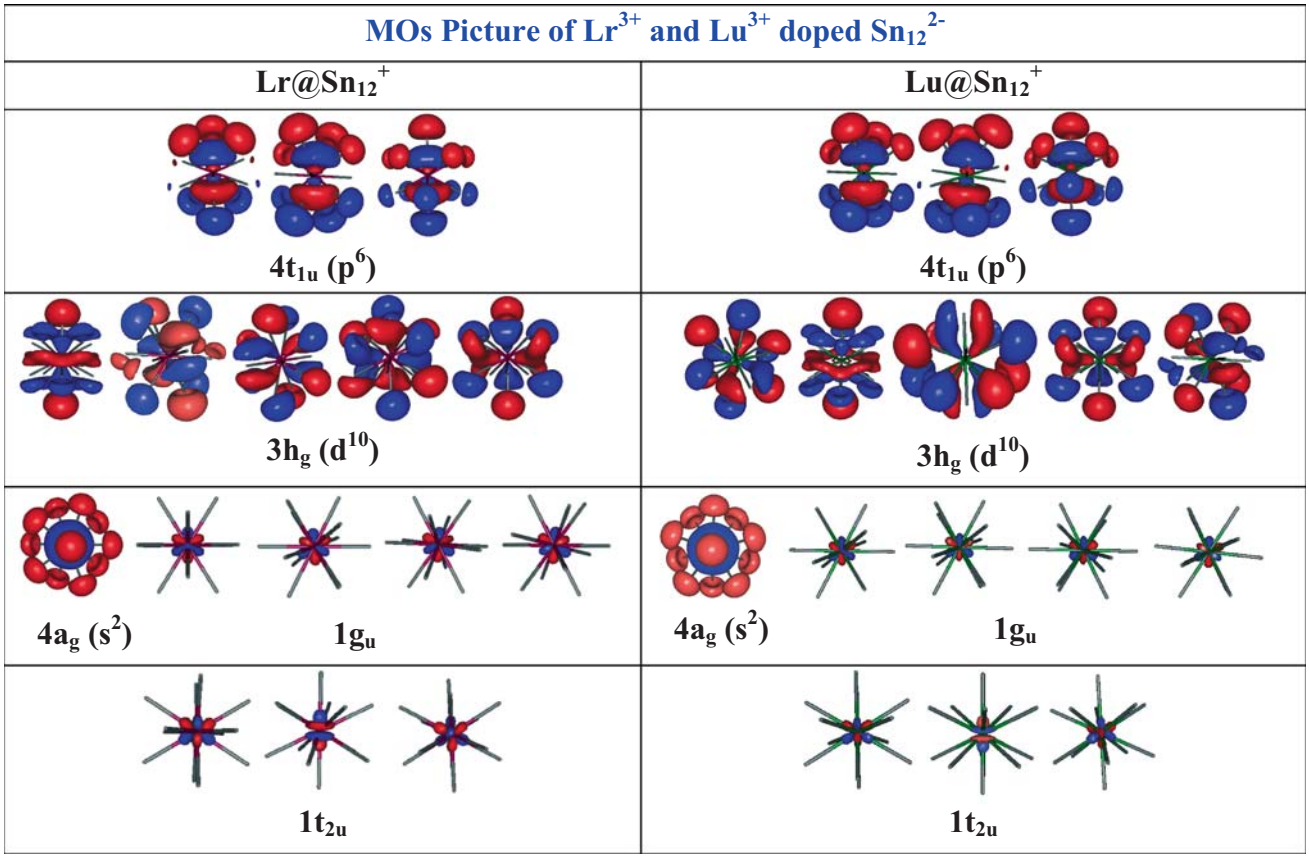

Figure 5. Molecular orbital pictures of $M@Sn_{12}^{+}$ clusters (M = Lr and Lu) at PBE/DEF level of theory. (Reproduced from Ref.[12] with permission from the Royal Society of Chemistry).

clusters, apart from these energy levels one additional higher energy state corresponding to $4t_{1u}$ MOs (HOMO) is generated due to the hybridization of the doped ion with the cage atom. Therefore, the HOMO-LUMO gap in the metal-doped cluster is reduced. On the other hand, early lanthanide or actinide encapsulated clusters such as $Pu@Pb_{12}$,[47,53] $[U@Si_{20}]^{6-}$,[73] $M@C$[26,72] (M = lanthanide/actinide), $Pu@C_{24}$[74] and $U@C_{28}$,[75] follow the 32-electron principle due to the participation of f-electrons in the bonding. However, in the case of Lr and Lu, the 4f/5f orbitals are highly shielded and their participation in the bonding with the cage atoms is negligible (Figures 4 and 5). As a consequence of the 4f/5f orbital of Lu/Lr not participating in bonding with the cage atoms, these systems follow 18-electron rule similar to that of the $M@Pb_{12}^{+}$ and $M@Sn_{12}^{+}$ (M=La, Ac) (Figure 4).

7. Estimation of the charge and electron localisation function

The Voronoi charge present on the metal atoms/ions in the $M@Pb_{12}^{2-}$ and $M@Sn_{12}^{2-}$ (M = Lr^{n+} and Lu^{n+}n = 0, 1, 2, 3) clusters have been studied in order to shed light on the nature of bonding within the clusters. The charges on Lr and the cage atom are significantly different from the initial charges on Lr (+3) and on the cage (−2). The increase in the electron density around the encapsulated ion and a decrease in the electron density of the cage indicates that a transfer of electron density has occurred from the orbitals of the cage atoms to the central atoms. Moreover, similar charges are localised on Lr and Lu, suggesting that Lr and Lu are forming similar kinds of bonds with the surrounding cage atoms.

In order to gain more understanding on the nature of the M–Pb and Pb–Pb bonds, the electron localization function[77] (ELF) for $M@Pb_{12}^{+}$ (M = Lr, Lu, La and Ac) and $M@Sn_{12}^{+}$ clusters (M = Lr, Lu) have been obtained and corresponding ELF plots of $M@Pb_{12}^{+}$ are provided in Figure 6.[12] Similar ELF plots have been found for $M@Sn_{12}^{+}$ clusters.[12] It has been found that more localization of electrons occurs among the cage atoms than between the cage and the central metal ion. This is as expected of heteroatoms and indicates that the metal–cage bond possesses only weak covalent interaction. Further, the ELF of the M–Pb bond is found to be larger in Lu^{3+} and Lr^{3+} encapsulated Pb_{12}^{2-} cluster as compared to the La^{3+}

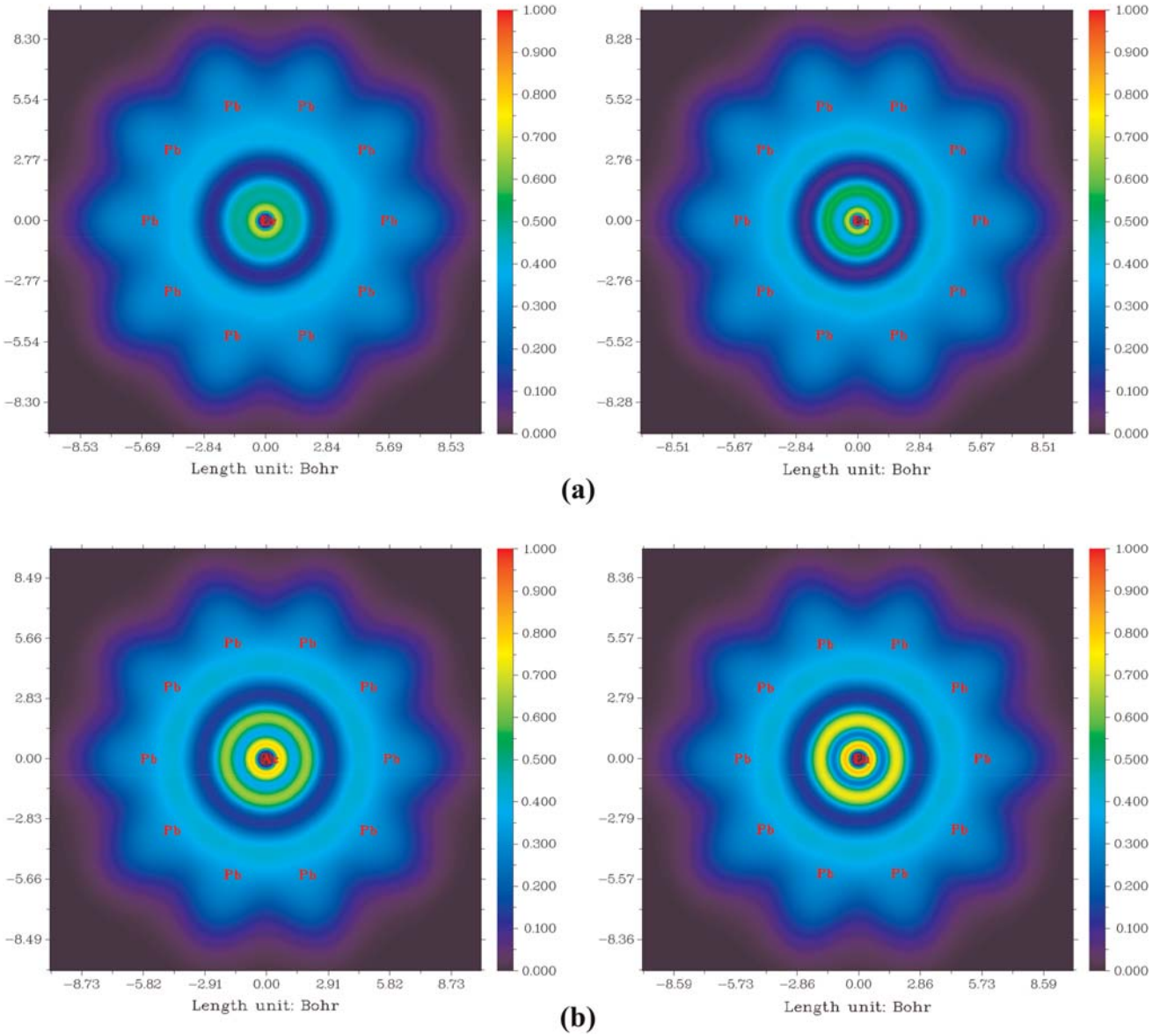

Figure 6. The 2−D colour−filled maps of the electron localization function (ELF) of (a) $Lr@Pb_{12}^{+}$ and $Lu@Pb_{12}^{+}$ (b) $Ac@Pb_{12}^{+}$ and $La@Pb_{12}^{+}$, respectively. (Reproduced from Ref.[12] with permission from the Royal Society of Chemistry).

and Ac^{3+} ion encapsulated Pb_{12}^{2-} cluster, indicating relatively less covalent character in the La^{3+} and Ac^{3+} ion encapsulated Pb_{12}^{2-} clusters. These observations corroborate with the trend in HOMO–LUMO energy gaps as well as those of binding energy.

8. Conclusions

The clusters considered in this computational study have negative values of binding energy combined with relatively large HOMO–LUMO energy gaps that indicate the stability of such encapsulated clusters. The optimized minimum energy structures and thus calculated parameters *viz.,* electronic, thermodynamic and geometric for Lr encapsulated clusters are in a close match with those parameters corresponding to Lu encapsulated clusters. Furthermore, the similarity between Lr and Lu metal atoms are manifested in their various oxidation states, though they possess different atomic ground state valence electronic configurations. It is all the more exciting to discover that La and Ac showed striking similarities to Lr and Lu with respect to all the properties investigated and also form stable 18-electron systems. The results of our study with adequate and corroborating justifications from its different perspectives showed that Lr^{3+}, Lu^{3+}, La^{3+}, and Ac^{3+} possess close similarities in their electronic

as well as structural behavior, favouring the placement of all the four of these elements together into 15 element f-block rows in agreement with Pyykkö and also the convention presently followed by the IUPAC.

Although the approach adopted by us has been a comprehensive and justified one there have been further discussions on this question as appeared[78] in "Chemistry World" as a news article, where Lavelle contradicted the 15-elements f-block rows. Further, Jemmis has expressed[79] that placing 15 elements in each of the f-blocks is inconsistent with the 14-element upper limit of occupancy of f-block. Moreover, he also pointed out[79] that many examples exist where similarities of actinides with that of the transition elements and similar behaviour of lanthanides with the main group elements are found. The periodic table as vital as it is to chemists of every kind is still a work in progress and is sure to attract more attention.[80] It could well be that more super-heavy elements are waiting to be discovered and extend the periodic table beyond the 118th element. We can, of course, continue to speculate about what could be in store for the periodic table in 150 years to come.

Acknowledgements

AC thanks SERB-DST for the post-doctoral fellowship. M.J. and T.K.G. gratefully acknowledge the liberal support provided by their host institution, Bhabha Atomic Research Centre, Mumbai. M. J. would like to thank Homi Bhabha National Institute for the PhD. fellowship in Chemical Sciences. It is a pleasure to thank Prof. E. D. Jemmis for many helpful discussions.

References

1. Jensen W B 1982 The positions of lanthanum (actinium) and lutetium (lawrencium) in the periodic table *J. Chem. Educ.* **59** 634
2. Jensen W B 2009 Misapplying the periodic law *J. Chem. Educ.* **86** 1186
3. Desclaux J-P and Fricke B 1980 Relativistic prediction of the ground state of atomic lawrencium *J. Phys.* **41** 943
4. Brewer L 1971 Energies of the electronic configurations of the lanthanide and actinide neutral atoms *J. Opt. Soc. Am.* **61** 1101
5. Fritzsche S, Dong C Z, Koike F and Uvarov A 2007 The low-lying level structure of atomic lawrencium (z = 103): energies and absorption rates *Eur. Phys. J. D.* **45** 107
6. Lavelle L 2008 Lanthanum (La) and actinium (ac) should remain in the d-block *J. Chem. Educ.* **85** 1482
7. Lavelle L 2009 Response to misapplying the periodic law *J. Chem. Educ*. **86** 1187
8. Lavelle L 2008 Response to the flyleaf periodic table *J. Chem. Educ*. **85** 1491
9. Xu W H and Pyykkö P 2016 Is the chemistry of lawrencium peculiar? *Phys. Chem. Chem. Phys.* **18** 17351
10. Sato T K, Asai M, Borschevsky A, Stora T, Sato N, Kaneya Y, Tsukada K, Düllmann C E, Eberhardt K, Eliav E, Ichikawa S *et al.* 2015 Measurement of the first ionization potential of lawrencium, element 103 *Nature* **520** 209
11. IUPAC, iupac.org/what−we−do/periodic−table−of−elements/, Downloaded. (2016)
12. Joshi M, Chandrasekar A and Ghanty T K 2018 Theoretical investigation of $M@Pb_{12}^{2-}$ and $M@Sn_{12}^{2-}$ zintl clusters (M = Lr^{n+}, Lu^{n+}, La^{3+}, Ac^{3+} and n = 0, 1, 2, 3) *Phys. Chem. Chem. Phys*. **20** 15253
13. TURBOMOLE is program package developed by the quantum chemistry group at the University of Karlsruhe, Germany, 1988: Ahlrichs R, Bär M, Häser M, Horn H and Kölmel C *Chem. Phys. Lett.*1989 **162** 165
14. ADF2016; SCM, Theoretical Chemistry, VrijeUniversiteit: Amsterdam, The Netherlands. http://www.scm.com
15. teVelde G, Bickelhaupt F M, van Gisbergen S A, Fonseca Guerra C, Baerends E J, Snijders J G and Ziegler T 2001 Chemistry with ADF *J. Comput. Chem.* **22** 931
16. Perdew J P, Burke K and Ernzerhof M 1996 Generalized gradient approximation made simple *Phys. Rev. Lett.* **77** 3865
17. Dolg M, Stoll H, Savin A and Preuss H 1989 Energy−adjusted pseudopotentials for the rare earth elements *Theor. Chim. Acta* **75** 173
18. Bergner A, Dolg M, Kuechle W, Stoll H and Preuss H 1993 Ab initio energy−adjusted pseudopotentials for elements of groups 13–17 *Mol. Phys.* **80** 1431
19. Dolg M, Stoll H and Preuss H 1993 A combination of quasirelativistic pseudopotential and ligand field calculations for lanthanoid compounds *Theor. Chim. Acta* **85** 441
20. Eichkorn K, Weigend F, Treutler O and Ahlrichs R 1997 Auxiliary basis sets for main row atoms and transition metals and their use to approximate coulomb potentials *Theor. Chem. Acc*. **97** 119
21. Kuechle W, Dolg M, Stoll H and Preuss H 1994 Energy-adjusted pseudopotentials for the actinides. parameter sets and test calculations for thorium and thorium monoxide *J. Chem. Phys.* **100** 7535
22. Cao X and Dolg M 2001 Valence basis sets for relativistic energy−consistent small−core lanthanide *J. Chem. Phys.* **115** 7348
23. Weigend F and Ahlrichs R 2005 Balanced basis sets of split valence, triple zeta valence and quadruple zeta valence quality for H to Rn: design and assessment of accuracy *Phys. Chem. Chem. Phys.* **7** 3297
24. Kroto H W, Heath J R, O'Brien S C, Curl R F and Smalley R E 1985 C_{60}: Buckminsterfullerene *Nature* **318** 162
25. Stark W J 2011 Nanoparticles in biological systems *Angew. Chem., Int. Ed.* **50** 1242
26. Daniel M C and Astruc D 2004 Gold nanoparticles: assembly, supramolecular chemistry, quantum–size–related properties, and applications toward biology, catalysis, and nanotechnology *Chem. Rev.* **104** 293

27. Luo Z, Castleman A W Jr and Khanna S N 2016 Reactivity of metal clusters *Chem. Rev.* **116** 14456
28. Jin R, Zeng C, Zhou M and Chen Y 2016 Atomically precise colloidal metal nanoclusters and nanoparticles: fundamentals and opportunities *Chem. Rev.* **116** 10346
29. Yadav B C and Kumar R 2016 Structure, properties and applications of fullerene *Int. J. Nanotechnol. Appl.* **2** 15
30. Chen X, Deng K, Liu Y, Tang C, Yuan Y, Hu F, Wu H, Huang D, Tan W and Wang X 2008 The geometric and magnetic properties of the endohedral plumbaspherene $M@Pb_{12}$ clusters (M = Sc, Ti, V, Cr, Mn, Fe, Co, Ni) *Chem. Phys. Lett.* **462** 275
31. Lichtenberger N, Wilson R J, Eulenstein A R, Massa W, Clérac R, Weigend F and Dehnen S 2016 Main Group metal–actinide magnetic coupling and structural response upon U^{4+} inclusion into Bi, Tl/Bi or Pb/Bi cage *J. Am. Chem. Soc.* **138** 9033
32. Manzoor D and Pal S 2015 Reactivity and catalytic activity of hydrogen atom chemisorbed silver cluster *J. Phys. Chem. A* **119** 6162
33. Cui L-F, Huang X, Wang L-M, Zubarev D Y, Boldyrev A I, Li J and Wang L-S 2006 Sn_{12}^{2-}: Stannaspherene *J. Am. Chem. Soc.* **128** 8390
34. Cui L-F, Huang X, Wang L-M, Li J and Wang L-S 2006 Pb_{12}^{2-}: Plumbaspherene *J. Phys. Chem. A* **110** 10169
35. Zhang X, Li G, Xing X, Zhao X, Tang Z and Gao Z 2001 Formation of binary alloy cluster anions from group–14 elements and cobalt and comparison with solid state Alloys *Rapid Commun. Mass Spectrom.* **15** 2399
36. Bai J 2003 Synthesis of inorganic fullerene−like molecules *Science* **300** 781
37. Esenturk E N, Fettinger J, Lam, Y-F and Eichhorn B 2004 $[Pt@Pb_{12}]^{2-}$ *Angew. Chem., Int. Ed.* **43** 2132
38. Esenturk E N, Fettinger J and Eichhorn B 2005 The closo−Pb_{10}^{2-}zintl ion in the $[Ni@Pb_{10}]^{2-}$ cluster *Chem. Commun.* 247
39. Spiekermann A, Hoffmann S D and Fässler T F 2006 The Zintl ion $[Pb_{10}]^{2-}$: A rare example of a homoatomiccloso cluster *Angew. Chem., Int. Ed.* **45** 3459
40. Esenturk E N, Fettinger J and Eichhorn B 2006 The Pb_{12}^{2-} and Pb_{10}^{2-}zintl ions and the $M@Pb_{12}^{2-}$ and $M@Pb_{10}^{2-}$ cluster series where M = Ni, Pd, Pt *J. Am. Chem. Soc.* **128** 9178
41. Reveles J U and Khanna S N 2006 Electronic counting rules for the stability of metal–silicon clusters *Phys. Rev. B* **74** 035435
42. Cui L F, Huang X, Wang L M, Li J and Wang L S 2007 Endohedral stannaspherenes $M@Sn_{12}^{-}$: a rich class of stable molecular cage clusters *Angew. Chem., Int. Ed.* **46** 742
43. Koyasu K, Atobe J, Furuse S and Nakajima A 2008 Anion photoelectron spectroscopy of transition metal– and lanthanide metal–silicon clusters: MSi_n^- (n = 6–20) *J. Chem. Phys.* **129**2 14301
44. Atobe J, Koyasu K, Furuse S and Nakajima A 2012 Anion photoelectron spectroscopy of germanium and tin clusters containing a transition− or lanthanide−metal atom, MGe_n^- (n = 8–20) and MSn_n^- (n = 15–17) (M = Sc–V, Y–Nb, and Lu–Ta) *Phys. Chem. Chem. Phys.* **14** 9403
45. Cao T-T, Zhao L-X, Feng X-J, Lei Y-M and Luo Y-H 2009 Structural and electronic properties of $LuSi_n$ (n = 1–12) clusters: a density functional theory investigation *J. Mol. Struct. TheoChem.* **895** 148
46. Fässler T F and Hoffmann S D 2004 Endohedral zintl ions: intermetalloid clusters *Angew. Chem., Int. Ed.* **43** 6242
47. Dognon J-P, Clavaguera C and Pyykkö P 2007 Towards a 32–electron principle: $Pu@Pb_{12}$ and related systems *Angew. Chem., Int. Ed.* **46** 1427
48. Kong X-J, Ren Y-R, Long L-S, Zheng Z, Huang R-B and Zheng L-S 2007 A keplerate magnetic cluster featuring an icosidodecahedron of Ni(II) ions encapsulating a dodecahedron of La(III) ions *J. Am. Chem. Soc.* **129** 7016
49. Kandalam A K, Chen G and Jena P 2008 Unique magnetic coupling between Mn doped stannaspherenes $Mn@Sn_{12}$ *Appl. Phys. Lett.* **92** 143109
50. Rohrmann U and Schäfer R 2015 Stren–Gerlach experiments on $Fe@Sn_{12}$: magnetic response of a jahn–teller distorted endohedrally doped molecular cage cluster *J. Phys. Chem. C* **119** 10958
51. Wang J-Q, Stegmaier S, Wahl B and Fässler T F 2010 Step–by–step synthesis of the endohedral stannaspherene $[Ir@Sn_{12}]^{3-}$ via the capped cluster anion $[Sn_9Ir(cod)]^{3-}$ *Chem. Eur. J.* **16** 1793
52. Rohrmann U and Schäfer R 2013 Stern–Gerlach experiments on $Mn@Sn_{12}$: identification of a paramagnetic superatom and vibrationally induced spin orientation *Phys. Rev. Lett.* **111** 133401
53. Dognon J-P, Clavaguéra C and Pyykkö P 2010 Chemical properties of the predicted 32–electron systems $Pu@Sn_{12}$ and $Pu@Pb_{12}$ *C. R. Chim.* **13** 884
54. Zhou B, Krämer T, Thompson A L, McGrady J E and Goicoechea J M 2011 A highly distorted open–shell endohedral zintl cluster: $[Mn@Pb_{12}]^{3-}$ *Inorg. Chem.* **50** 8028
55. Grubisic A, Wang H, Li X, Ko Y J, Kocak F S, Pederson M R, Bowen K H and Eichhorn B W 2011 Photoelectron spectroscopic and computational studies of the $Pt@Pb_{10}^{1-}$ and $Pt@Pb_{12}^{1-/2-}$ anions *Proc. Natl. Acad. Sci. U.S.A.* **108** 14757
56. Bhattacharyya S, Nguyen T T, Haeck K, Lievens P and Janssens E 2013 Mass–selected photodissociation studies of $AlPb_n^+$ clusters (n = 7–16): evidence for the extraordinary stability of $AlPb_{10}^+$ and $AlPb_{12}^+$ *Phys. Rev. B* **87** 054103
57. Kong X-J, Ren Y-R, Long L-S, Zheng Z, Nicol G, Huang R-B and Zheng L-S 2008 Dual shell−like magnetic clusters containing Ni^{II} and Ln^{III} (Ln = La, Pr, and Nd) ions *Inorg. Chem.* **47** 2728
58. Penga Q and Shen J 2008 Growth behavior of $La@Si_n$ (n = 1–21) metal-encapsulated clusters *J. Chem. Phys.* **128** 084711
59. Sekhar P, Ghosh A, Joshi M and Ghanty T K 2017 Noble gas encapsulated endohedral zintl ions $Ng@Pb_{12}^{2-}$ and $Ng@Sn_{12}^{2-}$ (Ng = He, Ne, Ar, and Kr): a theoretical investigation *J. Phys. Chem. C* **121** 11932
60. Srivastava A K, Pandey S K and Misra N 2016 Encapsulation of lawrencium into C_{60} fullerene: $Lr@C_{60}$ versus $Li@C_{60}$ *Mater. Chem. Phys.* **177** 437

61. Shao N, Bulusu S and Zeng X C 2008 Search for lowest-energy structure of zintldianion Si_{12}^{2-}, Ge_{12}^{2-}, and Sn_{12}^{2-} *J. Chem. Phys.* **128** 154326
62. Li X, Kiran B, Li J, Zhai H-J and Wang L-S 2002 Experimental observation and confirmation of icosahedral $W@Au_{12}$ and $Mo@Au_{12}$ molecules *Angew. Chem., Int. Ed.* **41** 4786
63. Pyykkö P and Runeberg N 2002 Icosahedral WAu_{12}:a predicted closed-shell species, stabilized by aurophilic attraction and relativity and in accord with the 18-electron rule *Angew. Chem., Int. Ed.* **12** 2174
64. Li L-J, Pan F-X, Li F-Y, Chen Z-F and Sun Z-M 2017 Synthesis, characterization and electronic properties of an endohedral plumbaspherene $[Au@Pb_{12}]^{3-}$ *Inorg. Chem. Front.* **4** 1393
65. Langmuir I 1921 Types of valence *Science* **54** 59
66. Pyykkö P 2006 Understanding the eighteen–electron rule *J. Organomet. Chem*. **691** 4336
67. deHeer W A 1993 The physics of simple metal clusters: experimental aspects and simple models *Rev. Mod. Phys.* **65** 611
68. Luo Z and Castleman A W 2014 Special and general superatoms *Acc. Chem. Res.* **47** 2931
69. Autschbach J, Hess B A, Johansson M P, Neugebauer J, Patzschke M, Pyykkö P, Reiher M and Sundholm D 2004 Properties of WAu_{12} *Phys. Chem. Chem. Phys.* **6** 11
70. Cao G-J, Schwarz W H E and Li J 2015 An 18–electron system containing a superheavy element: theoretical studies of $Sg@Au_{12}$ *Inorg. Chem.* **54** 3695
71. Dognon J P, Clavaguéra C and Pyykkö P 2009 A predicted organometallic series following a 32–electron principle: $An@C_{28}$ (An = Th, Pa^{+}, U^{2+}, Pu^{4+}) *J. Am. Chem. Soc.* **131** 238
72. Manna D and Ghanty T K 2012 Prediction of a new series of thermodynamically stable actinide encapsulated fullerene systems fulfilling the 32–electron principle *J. Phys. Chem. C* **116** 25630
73. Dognon J P, Clavaguéra C and Pyykkö P 2012 A new, centered 32–electron system: the predicted $[U@Si_{20}]^{6-}$–like isoelectronic series *Chem. Sci.* **3** 2843
74. Manna D, Sirohiwal A and Ghanty T K 2014 $Pu@C_{24}$: A new example satisfying the 32–electron principle *J. Phys. Chem. C* **118** 7211
75. Dai X, Gao Y, Jiang W, Leiab Y and Wang Z 2015 $U@C_{28}$: The electronic structure induced by the 32–electron principle *Phys. Chem. Chem. Phys.* **17** 23308
76. Muñoz–Castro A 2013 Golden endohedral main–group clusters, $[E@Au_{12}]^{q-}$: theoretical insights into the 20–e principle *J. Phys. Chem. Lett.* **4** 3363
77. Becke A D and Edgecombe K E 1990 A simple measure of electron localization in atomic and molecular systems *J. Chem. Phys.* **92** 5397
78. Walshe A 2018 Chemistry World. Accessed on 21-May: https://www.chemistryworld.com/news/new-rationale-for-15-element-wide-f-block/3009047.article
79. Jemmis E D 2018 Controversy continues on the position of elements in the periodic table *Curr. Sci.* **114** 2428
80. Lemonick S 2019 Rearranging the table *Chem. Eng. News.* **97** 26